

# Fluid-Free-Surface Proximity Effect on a Sphere Vertically Accelerated from Rest

J. G. WAUGH\*

*Naval Undersea Research and Development Center, San Diego, Calif.*

AND

A. T. ELLIS†

*University of California, San Diego, La Jolla, Calif.*

Apparatus was designed to determine the effect of free-surface proximity on the initial added mass, before boundary-layer separation, of a 1-in.-diam sphere accelerated vertically upward from rest in water. The sphere was accelerated electromagnetically, thereby avoiding generation of body elastic waves and extraneous fluid disturbances and making feasible relatively high accelerations over very short distances. Tests were conducted for a range of sphere center depths of 0.5 to 2.5 diameters. The data were compared with ideal fluid theory based on the assumption that the acceleration regime is sufficiently brief that inertial forces predominate and gravitational forces may be neglected. The results indicate that although there are slight viscous and gravitational effects over the acceleration regime, the agreement between experiment and theory is good.

## Nomenclature

$a$	= radius of sphere
$c$	= radius of accelerating coil
$C$	= capacity of accelerating circuit capacitor bank
$D$	= viscous drag on sphere due to wall shear stress
$E$	= initial potential of accelerating circuit capacitor bank
$F_a$	= magnetic accelerating force on sphere in air
$F_w$	= magnetic accelerating force on sphere in water
$F_v$	= magnetic accelerating force on sphere
$g$	= gravitational acceleration
$G_a$	= gravitational force on sphere
$G_w$	= negative buoyancy force on sphere in water
$h_\nu$	= doublet vertical positions or distances from fluid surface; $h_\nu$ is negative for primary sphere and positive for surface image doublet positions ( $\nu = 0, 1, 2, \dots$ )
$h_0$	= depth of primary sphere doublet
$I$	= current in accelerating coil
$K$	= initial added mass coefficient (ratio of added mass to mass of displaced fluid) of a sphere accelerated vertically from rest in water under a free surface
$K_0$	= initial added mass coefficient (ratio of added mass to mass of displaced fluid) of a sphere accelerated vertically from rest in an ideal fluid under a free surface ( $g = 0$ )

$K_\infty$	= initial added mass coefficient (ratio of added mass to mass of displaced fluid) of a sphere accelerated vertically from rest in an ideal fluid under a free surface ( $g = \infty$ )
$L$	= inductance of accelerating coil
$m$	= added mass of sphere
$M$	= mass of sphere
$N$	= number of turns of wire in accelerating coil
$r$	= resistance of accelerating circuit
$r_0$	= distance from primary sphere doublet
$r_\nu$	= distance from $\nu$ th primary sphere image doublet ( $\nu = 0, 1, 2, \dots$ )
$R$	= distance from origin of a point in the fluid surface ( $x, z$ plane)
$s_\nu$	= distance from $\nu$ th surface image doublet ( $\nu = 0, 1, 2, \dots$ )
$t$	= time
$T$	= natural period of accelerating circuit
$T/2$	= duration of accelerating force
$U(\theta)$	= potential fluid flow velocity over sphere for unit fluid velocity
$U_a(t)$	= velocity of sphere in air; $U_a(0) = 0$ , $U_a(T/2)$ = velocity at end of accelerating force regime
$U(t)$	= velocity of sphere in water; $U(0) = 0$ , $U(T/2)$ = velocity at end of accelerating force regime
$\mathbf{v}$	= fluid velocity; $\mathbf{v} = -\nabla\phi$
$x, y, z$	= orthogonal fluid coordinate system (see Fig. 1)
$\alpha$	= damping constant of accelerating circuit
$\eta$	= distance of sphere center below accelerating coil center
$\theta$	= angle between primary sphere radial coordinate $r_0$ and vertical direction, $y$ axis (see Fig. 1)
$\nu$	= kinematic viscosity of fluid
$\rho$	= density of fluid
$\phi$	= velocity potential of fluid
$\phi_0$	= velocity potential of primary sphere doublet
$\omega$	= natural frequency of accelerating circuit

## Superscript

( )' = indicates nondimensionalization of a linear quantity by expressing it in terms of the sphere radius; e.g.,  $h'_\nu = h_\nu/a$

## Introduction

A MAJOR problem in the design of bodies moving through a fluid is the evaluation of the inertial resistance of the fluid when the body is accelerated. This inertial resistance affects the motion of the body and is usually described in

Presented as Paper 69-42 at the AIAA 7th Aerospace Sciences Meeting, New York, January 20-22, 1969; submitted February 11, 1969; revision received June 13, 1969. This work was supported by the Department of the Navy, Bureau of Naval Weapons, Contract N600(19)59368 to the California Institute of Technology and Task Assignment RRRE-04001/216-1/R009-01-01 to the U.S. Naval Ordnance Test Station (now the Naval Undersea Research and Development Center), Pasadena, Calif. The authors are indebted to S. B. Melsen, Defence Research Establishment, Suffield, Ralston, Alberta, Canada, for his assistance in the experimental studies, and to A. G. Fabula, Naval Undersea Research and Development Center, for his helpful advice and suggestions. The work reported in this paper was conducted by the authors in the Hydrodynamics Laboratory, California Institute of Technology, Pasadena, Calif.

\* Staff Scientist, Ocean Technology Department, Pasadena, Calif.; also Visiting Lecturer and Research Engineering Physicist, University of California, San Diego, La Jolla, Calif.

† Professor of Applied Mechanics, Department of Aerospace, Mechanical Engineering Sciences.

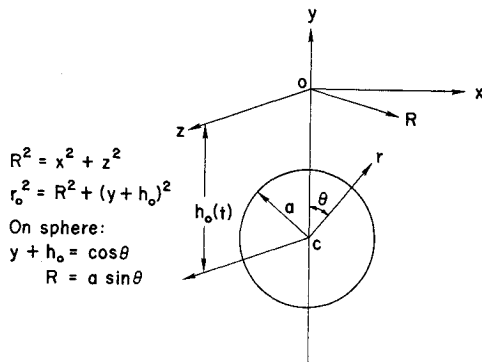


Fig. 1 Coordinate systems for fluid and sphere.

terms of an apparent increase in the mass (added mass) of the body.<sup>1</sup> Although in theory added masses can be computed for any flow situation and used to determine a complete expression for the ideal pressure forces, the actual solution of the problem often proves mathematically intractable. The greatest difficulties are found in the determination of motion of bodies not deeply submerged; that is, bodies close to a free surface.

It is known that potential frictionless flow exists in a real fluid during the first instant after a body is accelerated from rest.<sup>2</sup> Generally speaking, inertial resistance to acceleration from rest in a real fluid should agree with ideal fluid theory and quite good agreement has been obtained for a sphere when all solid boundaries are remote,<sup>1</sup> but no tests appear to have been made of this hypothesis for a body in the presence of a free surface. In this paper, studies to determine experimentally the initial added mass of a sphere accelerated vertically upward from rest at varied depths in water are described and the results compared with ideal fluid theory.

### Theory

In the following discussion, we assume an ideal fluid with orthogonal coordinate axes  $x, y, z$  such that the  $x, z$  plane lies in the undisturbed free fluid surface and the  $y$  axis is directed positively vertically upward (Fig. 1). Let the velocity potential which satisfies all boundary conditions be  $\phi(x, y, z, t)$ , the fluid velocity (assumed to be small everywhere) be  $\mathbf{v} = -\nabla\phi$ , and all disturbances arising from  $\phi$  be negligible at a great distance.

Now consider a disturbance generated in the fluid involving high fluid accelerations, but considered over a sufficiently brief interval of time that fluid displacements and velocities are small. Then the gravitational effect will be negligible

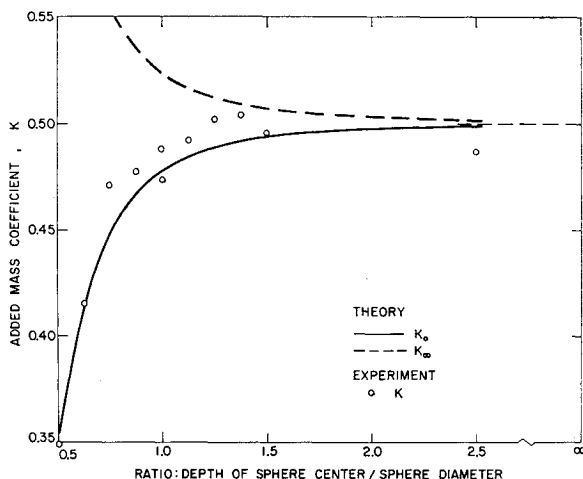


Fig. 2 Effect of water surface proximity on the added mass.

Table 1 Effect of depth of submergence on  $K_0$

Initial depth of sphere center, radii	Added mass coefficient, $K_0$
1	0.3521
1.1	0.3806
1.2	0.4038
1.3	0.4218
1.4	0.4360
1.5	0.4473
1.75	0.4661
2	0.4770
2.25	0.4837
2.5	0.4881
2.75	0.4910
3	0.4931
4	0.4970
5	0.4985
$\infty$	0.5000

and inertial forces will predominate. Under these assumptions, we obtain the free-surface high Froude-number boundary condition<sup>3</sup>:

$$\phi = 0 \quad (y = 0) \quad (1)$$

We consider, next, a sphere accelerated vertically upward from rest at different depths below the fluid surface. Referring to Fig. 1, the potential function for a sphere of radius  $a$  in fluid of infinite extent, moving upward along the  $y$  axis is

$$\phi_0 = \frac{U(t)a^3 \cos\theta}{2 r_0^2} = \frac{U(t)a^3 y + h_0(t)}{2 r_0^3} \quad (2)$$

where  $U(t)$  is the sphere velocity and  $h_0(t)$  is the instantaneous position of the center of the sphere below the origin. The boundary condition on the sphere is given by

$$-\partial\phi_0/\partial r_0 = U(t) \cos\theta \quad (r_0 = a) \quad (3)$$

With the above boundary conditions, using the classical technique of successive "image" doublets in the sphere and free surface,<sup>4</sup> the following initial instantaneous velocity potential is obtained (it will be useful later for estimating the drag impulse on the sphere):

$$\phi = \frac{U(t)a^3}{2} \left[ \frac{y + h_0}{r_0^3} + \sum_{p=1}^{\infty} (-1)^p \prod_{p=1}^p \left( \frac{a}{h_0 + h_{p-1}} \right)^3 \times \left( \frac{y + h_p}{r_p^3} \right) + \frac{y - h_0}{s_0^3} + \sum_{p=1}^{\infty} (-1)^p \prod_{p=1}^p \left( \frac{a}{h_0 + h_{p-1}} \right)^3 \times \left( \frac{y - h_p}{s_p^3} \right) \right] \quad (4)$$

where

$$h_p = h_0 - \frac{a^2}{h_0 + h_{p-1}} \quad (p = 1, 2, 3, \dots) \quad (5)$$

and

$$\begin{aligned} r_p^2 &= R^2 + (y + h_p)^2 \quad (\nu = 0, 1, 2, \dots) \\ s_p^2 &= R^2 + (y - h_p)^2 \quad (\nu = 0, 1, 2, \dots) \end{aligned} \quad (6)$$

The limit points of the image doublet positions are  $\pm(h_0^2 - a^2)^{1/2}$ .

Equation (4) is also the velocity potential of two spheres of radius  $a$ , separated by a distance  $2h_0$  between centers, accelerated equally from rest in the same direction in the line of centers in fluid of infinite extent. For fluid initially at rest, the impulsive pressure in generating the motion<sup>4</sup> is given by  $\rho\phi$ , and since from Eq. (4),  $\phi(-y, R) = -\phi(y, R)$ , it can be readily shown that the added mass of the sphere pair ac-

celerated in infinite fluid must be twice that of the sphere accelerated toward the free surface. The added mass coefficients that are based on the mass of fluid displaced would therefore be the same. Consequently, the added mass coefficients, corresponding to different sphere depths, may be conveniently obtained from Eq. (2) of Ref. 5, which has been deduced from the work of Shiffman and Spencer.<sup>6</sup> In the nomenclature of this paper

$$K_0 = \frac{3}{2} \left[ \sum_{\nu=1}^{\infty} (-1)^{\nu+1} \frac{\sin^2 \beta}{\sin^2 \nu \beta} - \frac{2}{3} \right], \quad \cos \beta = h'_0 \quad (7)$$

and  $\beta$  is imaginary. Values of  $K_0$  corresponding to various depths are given in Table 1 and  $K_0$  is shown plotted as function of sphere depth in Fig. 2.

The preceding theory is based on the assumption that  $g = 0$ , that is, only inertial forces are considered. If we set  $g = \infty$ , no surface deformation can take place and we have the case of a sphere moving vertically toward a rigid wall<sup>7</sup> for which the added mass coefficient (correct to terms in  $h_0^{-3}$ ) is given by

$$K_{\infty} = \frac{1}{2} + \frac{3}{2}(a/2h_0)^3 = \frac{1}{2} + \frac{3}{2}(1/2h'_0)^3 \quad (8)$$

where  $h_0$  is now the distance of the sphere center from the wall (fluid surface). The added mass coefficient is shown plotted as a function of sphere depth in Fig. 2. In experimental studies where sphere displacement and velocity are necessarily involved and  $0 < g < \infty$ , both viscous and gravitational effects would arise, and experimentally obtained added mass coefficients  $K$  should be greater than the corresponding theoretical values  $K_0$ , and even greater than  $K_{\infty}$  for sufficiently viscous liquids. Where a valid correction can be made for viscous effects, it seems reasonable to assume that  $K_0 < K < K_{\infty}$ .

### Apparatus

Important considerations in the proposed study were the avoidance of boundary-layer separation over the acceleration regime and extraneous hydrodynamic disturbances that could result from conventional propulsion methods. It was felt that very small initial disturbances could lead to variations in the subsequent boundary-layer flow which could significantly affect hydrodynamic forces on the model. An ideal solution would be the use of "action at a distance," whereby the sphere would be accelerated in the fluid without any material involvement.

A simple circular coil of wire with current flowing in it acting on a paramagnetic sphere centered on the axis of the coil, as shown in Fig. 3, was chosen as the propulsion system for the following reasons: 1) the magnitude and duration of the accelerating force could be easily adjusted; 2) it satisfied the condition of action at a distance; 3) it generated a "body" force, thereby avoiding body distortion and vibration; 4) the force was uniquely directed and purely translational without moment, acting through the center of gravity of the sphere.

We assume that the breadth and width of the windings of the coil shown in Fig. 3 are small compared to its radius. Let a solid homogeneous paramagnetic sphere, whose radius is small compared with the coil radius, be centered on the coil axis at a distance  $\eta$  below the coil center. Then it can be shown<sup>8</sup> that the magnetic force on the sphere, directed along the  $y$  axis toward the center of the coil is given by, approximately,

$$F_y \approx K' N^2 c^4 I^2 \eta / (c^2 + \eta^2)^4 \quad (9)$$

where  $K'$  is a constant. For a hollow sphere,  $K'$  would be different, but the space function would be the same. For maximum force,  $\eta = 0.378c$ .

The circuit for energizing the coil and thereby accelerating the sphere is shown in Fig. 4. It consists essentially of a

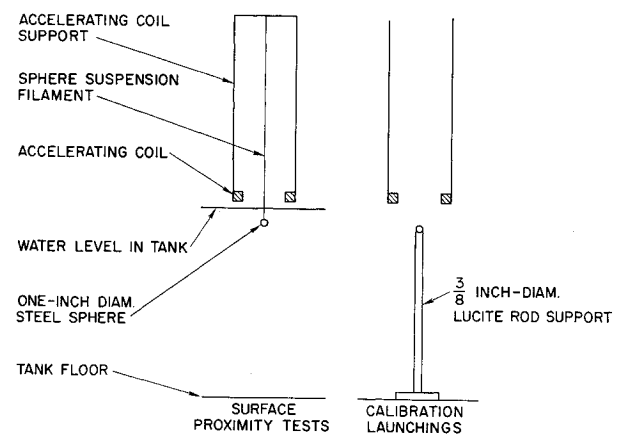


Fig. 3 Techniques used to accelerate sphere under water and in air.

capacitor bank which is given a predetermined charge and subsequently discharged through the coil by means of an ignitron, an electrically controlled switch of low resistance and high current capacity. The ignitron will hold off potentials up to 20,000 v, but will conduct current in only one direction. Thus the current cannot reverse and will be a half-cycle of an underdamped sine wave, giving a single acceleration pulse. The period is determined by the circuit parameters, but if the current is not zero by the time the sphere passes the center of the coil, it will experience deceleration. The current is given by<sup>9</sup>

$$I = (E/\omega L)e^{-\alpha t} \sin \omega t, \quad \alpha = r/2L \quad (10)$$

and the angular frequency of oscillation by

$$\omega = [1/LC - (r/2L)^2]^{1/2} \quad (11)$$

The time is measured from the instant when the capacitor bank discharge through the coil is initiated, i.e., start of the acceleration regime.

The coil used in these tests consisted of 108 turns of 16-gauge aluminum wire with an o.d. of 7.1 in., an i.d. of 5.4 in., and a width of 0.7 in. Circuit parameters were as follows:  $r = 1.338 \Omega$  (coil resistance of  $0.938 \Omega$ ),  $L = 3.441$  mH, and  $C = 450 \mu\text{f}$ . The measured acceleration period was  $T/2 = 4.03$  ms,  $\omega = 779.8$  rad/sec, and  $\alpha = 194.4$  rad/sec. For all tests,  $E = 5800$  v with the sphere 3.5 in. below the coil. Since current discharge elevated the coil temperature about  $5^\circ\text{C}$ , an operating coil temperature of  $30 \pm 1^\circ\text{C}$  was used. This was about  $7^\circ\text{C}$  above ambient temperature, permitting the coil to cool to operating temperature in about 15 min after each test.

### Experiment

A highly polished hollow steel sphere was used in these studies. It was  $1.004 \pm 0.0001$  in. in diameter and weighted to 9.3055 g so that it was 0.6411 g negatively buoyant with respect to water at an ambient temperature of  $20^\circ\text{C}$ . The sphere displacement over the pulse interval was less than

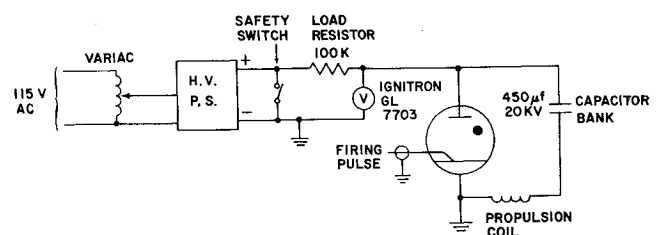


Fig. 4 Circuit for accelerating sphere.

$\frac{3}{16}$  in.; no rotation or cavitation was observable. By accelerating the sphere in water and in air under otherwise similar conditions, it was possible to determine its added mass.

For launchings in water, as shown in Fig. 3, the coil was positioned above the water surface to avoid hydrodynamic interference effects, and the sphere was positioned below the coil by means of a suspending thread. Varying sphere depths below the water surface were obtained by adjusting the water level. Since the negative buoyancy of the sphere was negligible, it was not necessary to consider any stored energy in the thread in the impulse to the sphere. For calibration launchings in air, where this would not be the case and where estimation of the energy in the thread would be uncertain, the sphere was supported by a Lucite rod. Because of hydrodynamic interference, a supporting rod could not be used in the tests with water. Tests were conducted in the test section of a nonmagnetic Lucite water tank<sup>10</sup> whose walls were at least 9 in. distant from the sphere; therefore, wall effects could be ignored. An optical technique was used to obtain sphere displacement-time data.<sup>11</sup> A more complete description of the electromagnetic accelerating technique, together with the theory involved, is given in Ref. 8.

Experimental data for sphere depths of 1.0, 1.5, and 2.5 diameters below the water surface are given in Table 2. For sphere accelerations in water, if we equate the total impulse acting on the sphere to the momentum change, we obtain

$$\int_0^{T/2} (F_w - D - G_w) dt = \int_0^{T/2} d[(M + m)]U = (M + m)U \left( \frac{T}{2} \right) \quad (12)$$

For the sphere launched in air, the impulse momentum relationship (the added mass is negligible) is

$$\int_0^{T/2} (F_a - G_a) dt = MU_a \left( \frac{T}{2} \right) \quad (13)$$

Defining the impulses by

$$I_a = \int_0^{T/2} F_a dt \quad (14)$$

and using Eqs. (12) and (13), the following relationship can be deduced:

$$\frac{m}{M} = \frac{1}{U(T/2)} \left[ \frac{U_a(T/2) + I_{Ga}/M}{I_{Fa}/I_{Fw}} - \frac{I_D}{M} - \frac{I_{Gw}}{M} \right] - 1 \quad (15)$$

Now the magnetic propulsive force on the sphere is not only a function of time but also a function of sphere position. Since the acceleration of the sphere will be greater in air than in water, its displacement toward the coil for corresponding times during the pulse period will be greater and its impulse greater. This difference in impulse was estimated by measuring the sphere displacement-time records and numerically integrating the data, making use of electromagnetic theory given in Ref. 8. For the data presented in Table 2, the impulse ratio  $I_{Fa}/I_{Fw} = 1.002$ . The pulse duration,  $T/2$ , was about 4.03 ms and  $g = 386.1$  in./sec<sup>2</sup>. For launchings in air, the sphere left the supporting rod 0.08 ms after pulse initiation,<sup>8</sup> but the correction to the magnetic force impulse due to this was found to be negligible. Therefore  $I_{Ga}/M = 1.52$  in./sec. Now  $M = 9.3055$  g and  $G_w = 0.6411$  g, from which  $I_{Gw} = 0.107$  in./sec.

In order to compute the drag impulse  $I_D$ , we will assume that boundary-layer separation did not occur over the acceleration regime, and flow outside the boundary layer was potential or very nearly so. Later we will show that these assumptions are justified. Referring to Eq. (4), the principal contribution to the velocity potential is given by the primary

**Table 2 Effect of depth of submergence on  $K$**

Parameter	Launchings in water sphere center depth, diam			Launchings in air
	2.5	1.5	1.0	
$U(T/2)$ , in./sec	52.73	53.03	52.95	76.03
	52.53	51.80	53.29	75.75
	52.35	52.35	53.02	75.83
	51.99	52.29	52.85	75.16
	53.04	51.95	52.61	75.14
Av. $U(T/2)$ , in./sec	52.528	52.267	52.991	75.49
Av. $K$	0.487	0.495	0.474	75.567
Av. $K$ limits (95.46%)	0.475	0.483	0.465	
Av. $K$ limits (99.73%)	0.469	0.477	0.461	
	0.506	0.513	0.486	

sphere and first surface and sphere image doublets; the contributions of succeeding doublets diminish rapidly, especially at greater depths. We obtain, then, the approximate velocity potential for fluid flow,

$$\phi = \frac{U(t)a^3}{2} \left[ \frac{\cos\theta}{r_0^2} - \frac{1}{(2h_0)^2} - \frac{2r_0 \cos\theta}{(2h_0)^3} - \left( \frac{a}{2h_0} \right)^3 \frac{\cos\theta}{r_0^2} \right] + U(t)r_0 \cos\theta \quad (16)$$

Then the fluid velocity outside the boundary layer over the sphere is given by

$$-(\partial\phi/r_0\partial\theta)_{r_0=a} = [3U(t)/2][1 - 1/(2h'_0)^3] \sin\theta \quad (17)$$

Equation (17) indicates that depth has only a slight effect on the initial flow over the sphere on starting from rest. For unit velocity, from Eq. (17),

$$U(\theta) = \frac{3}{2}[1 - 1/(2h'_0)^3] \sin\theta \quad (18)$$

From theory (Refs. 8 and 12), the drag impulse is given by

$$I_D = 2\rho \left( \frac{\nu}{\pi} \right)^{1/2} \int_0^\pi 2\pi a^2 \sin^2\theta U(\theta) d\theta \times \left[ U(T/2) \int_0^{T/2} \left( \frac{T}{2} - \tau \right)^{1/2} e^{-2\alpha\tau} \sin^2\omega\tau d\tau / \int_0^{T/2} e^{-2\alpha\tau} \sin^2\omega\tau d\tau \right] \quad (19)$$

where  $\rho = 0.998$  g/cm<sup>3</sup> and  $\nu = 1.007 \times 10^{-2}$  cm<sup>2</sup>/sec at 20°C,  $a = 0.502$  in., and  $U(T/2)$  is the velocity of the sphere at the end of the pulse regime in inches per second. The units of measurement have been mixed for convenience. In the laboratory, the scale used for weighing was calibrated in grams and measurements of distances were made in inches.

**Table 3 Effect of depth of submergence on  $K$**

Sphere center depth, diam	Average $K^a$	Fiducial limits for $K$	
		95.46%	99.73%
$\frac{1}{2}$	0.348	$\pm 0.009$	$\pm 0.013$
$\frac{5}{8}$	0.415	$\pm 0.006$	$\pm 0.009$
$\frac{3}{4}$	0.471	$\pm 0.015$	$\pm 0.023$
$\frac{7}{8}$	0.477	$\pm 0.006$	$\pm 0.009$
1	0.488	$\pm 0.006$	$\pm 0.009$
$1\frac{1}{8}$	0.492	$\pm 0.006$	$\pm 0.009$
$1\frac{1}{4}$	0.502	$\pm 0.007$	$\pm 0.010$
$1\frac{3}{8}$	0.504	$\pm 0.005$	$\pm 0.007$

<sup>a</sup> Obtained from six tests at each depth.

Drag impulses for various sphere depths were calculated from Eqs. (18) and (19) and the values of  $U(T/2)$  are given in Table 2. The integral in the numerator of Eq. (19) was evaluated by Simpson's rule and was found to be  $4.214 \times 10^{-8} \text{ sec}^{3/2}$ . The other two integrals are easily evaluated, the left-hand integral (considering only the integrand  $\sin^3\theta$ ) having the value  $\frac{4}{3}$  and the integral in the denominator the value  $9.670 \times 10^{-4} \text{ sec}$ . The results show that  $I_D = 5.28, 5.23, \text{ and } 5.25 \text{ g-in./sec}$  for sphere depths of 2.5, 1.5, and 1.0 diameters, respectively. Substituting these values and the values of  $U_a(T/2)$  and  $U(T/2)$  from Table 2 into Eq. (15), we obtain  $m/M$ , the added-mass-to-sphere-mass ratio. The mass of fluid displaced by the sphere is  $M - G_w = 9.3055 - 0.6411 = 8.6644 \text{ g}$ , and therefore  $M/(M - G_w) = 1.0740$ . Multiplying  $m/M$  by this factor, we obtain  $m/(M - G_w) = K$ , the added mass coefficient.

For a comparison of theory and experiment to be valid, it is necessary to show that boundary-layer separation did not occur and fluid flow outside the boundary layer was essentially potential over the acceleration regime. The maximum (final) Reynolds number is  $3.41 \times 10^4$ , well below the critical ( $3 \times 10^5$ ), and laminar boundary-layer flow should obtain. E. Boltze<sup>2</sup> showed that the distance traveled by a sphere launched impulsively from rest before separation starts is  $S = 0.392a$ . H. Blasius<sup>2</sup> showed in the case of two-dimensional flow that separation occurs at longer distances from the starting point for constant acceleration than for motion started impulsively. In brief, motion that is started impulsively appears to be the worst case. In these tests,  $a = 0.502 \text{ in.}$  and if the motion were started impulsively,  $S$  would be 0.197 in. From data measurements, the displacement of the sphere during the force pulse was at most 0.188 in., and since its acceleration was a damped half-sine wave with respect to time, the sphere must have traveled some distance after pulse termination before separation began.

Added mass coefficients have been calculated from the data of Table 2, making use of the above theory. They are also presented in Table 2 together with fiducial limits corresponding to the 0.9546 and 0.9973 probability levels. These were calculated from statistical theory given in Ref. 8. Added mass coefficients obtained under similar conditions<sup>8</sup> have been subsequently corrected for the drag impulse and their fiducial limits calculated. These data, given in Table 3, are more reliable than those of Table 2, for they were obtained at a later time when more precise techniques for positioning the sphere with respect to the coil had been developed and electrical instrumentation for more accurately controlling launching conditions had been obtained. This probably accounts for the data of Table 2 being consistently below those of Table 3 and the low experimental value for a sphere depth of 2.5 diameters.

### Discussion and Conclusions

The data of Tables 1 and 2, which are illustrated in Fig. 2, show good agreement between theory ( $K_0$ ) and experiment.

In no case did the experimental results and theory deviate significantly (0.9546 probability level), although the deviation for a depth of 2.5 sphere diameters is close to this level.

The data of Tables 1 and 3, also illustrated in Fig. 2, show good agreement for sphere depths of  $\frac{1}{2}$  and  $\frac{3}{8}$  diameters, but deviate significantly (0.9546 probability level) for a depth of  $1\frac{1}{8}$  diameters and highly significantly (0.9973 probability level) for depths of  $\frac{3}{4}, \frac{7}{8}, 1, 1\frac{1}{4}, \text{ and } 1\frac{3}{8}$  diameters.

From Fig. 2, it is seen that these significant deviations all lie above the theoretical curve for  $K_0$  and below the theoretical curve for  $K_\infty$ , indicating that there may have been some gravitational effect during the acceleration regime. However, the good agreement between theory ( $K_0$ ) and experiment from the standpoint of over-all added mass coefficient values indicates that the theory provides a good approximation to the experimental initial added mass.

It is concluded that for briefer acceleration regimes, viscous and gravitational effects would decrease and the agreement between theory and experiment would improve. A short-duration impulse is therefore essential and special experimental techniques such as described herein must be used.

### References

- <sup>1</sup> Birkhoff, G., *Hydrodynamics*, Princeton University Press, Princeton, N.J., 1960, Chap. 6.
- <sup>2</sup> Schlichting, H., *Boundary Layer Theory*, 4th ed., McGraw-Hill, New York, 1960, pp. 120, 185, 218-221.
- <sup>3</sup> Robertson, J. M., *Hydrodynamics in Theory and Application*, Prentice-Hall, Englewood Cliffs, N.J., 1965, pp. 284-285.
- <sup>4</sup> Lamb, H., *Hydrodynamics*, 6th ed., Dover, New York, 1945, pp. 46, 130-131.
- <sup>5</sup> Sarpkaya, T., "Added Mass of Lenses and Parallel Plates," *Journal of the Engineering Mechanics Division, Proceedings of the American Society of Civil Engineers*, Vol. 86, No. EM 3, June 1960, pp. 141-152.
- <sup>6</sup> Shiffman, M. and Spencer, D. C., "Flow of Incompressible Fluid about a Lens," *Quarterly of Applied Mathematics*, Vol. 5, No. 3, 1947, pp. 270-288.
- <sup>7</sup> Milne-Thompson, L. M., *Theoretical Hydrodynamics*, 2nd ed., Macmillan and Co., London, England, 1949, Chap. 16, pp. 446-447.
- <sup>8</sup> Mellisen, S. B., Ellis, A. T., and Waugh, J. G., "On the Added Mass of a Sphere in a Circular Cylinder Considering Real Fluid Effects," Rept. E-124.1, March 1966, Hydrodynamics Lab., California Institute of Technology.
- <sup>9</sup> Page, L. and Adams, N. I., *Principles of Electricity*, Van Nostrand, New York, 1931, pp. 352-353.
- <sup>10</sup> Waugh, J. G. and Ellis, A. T., "The Variable-Atmosphere Wave Tank," *Cavitation Research Facilities and Techniques*, American Society of Mechanical Engineers, 1964.
- <sup>11</sup> Waugh, J. G., Ellis, A. T., and Mellisen, S. B., "Techniques for Metric Photography," *Journal of the Society of Motion Picture and Television Engineers*, Vol. 75, No. 1, Jan. 1966, pp. 2-6.
- <sup>12</sup> Mellisen, S. B., Waugh, J. G., and Ellis, A. T., "Real Fluid Effects on an Accelerated Sphere Before Boundary-Layer Separation," Paper 66-WA/UNT-6, 1966, American Society of Mechanical Engineers.